

This is the peer reviewed version of the following article:

CD69 targeting enhances anti-Vaccinia virus immunity

Laura Notario, Jennifer Redondo-Antón, Elisenda Alari-Pahissa, Almudena Albentosa,  
Magdalena Leiva, Daniel Lopez, Guadalupe Sabio, Pilar Lauzurica1

J Virol . 2019 Sep 12;93(19):e00553-19.

which has been published in final form at

<https://doi.org/10.1128/JVI.00553-19>

# CD69 targeting enhances anti-Vaccinia virus immunity

Laura Notario<sup>1</sup>, Jennifer Redondo-Antón<sup>1</sup>, Elisenda Alari-Pahissa<sup>2</sup>, Almudena Albentosa<sup>1</sup>, Magdalena Leiva<sup>3</sup>, Daniel Lopez<sup>1</sup>, Guadalupe Sabio<sup>3</sup>, Pilar Lauzurica<sup>1</sup>

<sup>1</sup> Microbiology National Center, Instituto de Salud Carlos III, Majadahonda, Madrid, Spain.

<sup>2</sup> Currently in Universitat Pompeu Fabra, Barcelona, Spain

<sup>3</sup> Fundación Centro Nacional de Investigaciones Cardiovasculares Carlos III, Madrid, Spain

Address correspondence to: Dr. Pilar Lauzurica, Immunology Department, Microbiology National Center, Instituto de Salud Carlos III, Majadahonda 28220, Madrid, Spain. Phone: +34 918223718; Fax number: +34 915097919; E-mail: [lauzurica@isciii.es](mailto:lauzurica@isciii.es).

<http://orcid.org/0000-0001-6579-1948>

**Running title:** Anti-CD69 therapy increase VACV immune response

**Keywords:** Vaccinia virus, mAb, immunotherapy, innate immunity, infection clearance.

2 **Abstract**

3 CD69 is highly expressed on the leukocyte surface upon viral infection, and its  
4 regulatory role in the vaccinia virus (VACV) immune response has been recently  
5 demonstrated using CD69<sup>-/-</sup> mice. Here, we show augmented control of VACV infection  
6 using the anti-human CD69 monoclonal antibody (mAb) 2.8 as both preventive and  
7 therapeutic treatment for mice expressing human CD69. This control was related to  
8 increased natural killer (NK) cell reactivity and increased numbers of cytokine-  
9 producing T and NK cells in the periphery. Moreover, similarly increased immunity and  
10 protection against VACV were reproduced over both long and short periods in anti-  
11 mouse CD69 mAb 2.2-treated immunocompetent wild-type (WT) mice and  
12 immunodeficient Rag2<sup>-/-</sup> CD69<sup>+/+</sup> mice. This result was not due to synergy between  
13 infection and anti-CD69 treatment since, in the absence of infection, anti-human CD69  
14 targeting induced immune activation, which was characterized by mobilization,  
15 proliferation, and enhanced survival of immune cells as well as marked production of  
16 several innate proinflammatory cytokines by immune cells. Additionally, we showed  
17 that the rapid leukocyte effect induced by anti-CD69 mAb treatment was dependent on  
18 mTOR signaling. These properties suggest the potential of CD69-targeted therapy as an  
19 antiviral adjuvant to prevent derived infections.

20

21 **Importance**

22 In this study, we demonstrate the influence of human and mouse anti-CD69 therapies on  
23 the immune response to VACV infection. We report that targeting CD69 increases the  
24 leukocyte numbers in the secondary lymphoid organs during infection and improves the  
25 capacity to clear the viral infection. Targeting CD69 increases the numbers of gamma  
26 interferon (IFN $\gamma$ )- and tumor necrosis factor alpha (TNF $\alpha$ )-producing NK and T cells.  
27 In mice expressing human CD69, treatment with an anti-CD69 mAb produces increases  
28 in cytokine production, survival and proliferation mediated in part by mTOR signaling.  
29 These results, together with the fact that we have mainly worked with a human-CD69  
30 transgenic model, reveal CD69 as a treatment target to enhance vaccine protectiveness.

## 31 **Introduction**

32 The use of vaccinia virus (VACV) had an essential role in the eradication of smallpox,  
33 and since then, VACV has been used as a model to study virus-host interactions. It is a  
34 complex, enveloped, linear, double-stranded DNA virus with many genes dedicated to  
35 the evasion of the innate immune system and the action of interferons. VACV infection  
36 clearance is first controlled by the innate immune response mostly through NK cells due  
37 to the production of cytokines such as type I and II IFNs and TNF $\alpha$  (1). However,  
38 ultimately, if VACV infection is not resolved, a powerful adaptive immune response  
39 essential for the proper elimination of VACV infection is activated by specific CD8+  
40 and CD4+ T cells (2). Currently, in many clinical trials, vaccinia virus is being used to  
41 construct directed targets for vaccine candidates against various diseases, such as  
42 HIV/AIDS (3), hepatitis (4), influenza (5), malaria (6), tuberculosis (7), and even  
43 oncogenic diseases of both human and domestic animals (8).

44 CD69 is a leukocyte receptor constitutively expressed on the surface of subsets of  
45 thymocytes, T cells, NK cells, plasmacytoid dendritic cells and progenitor cells (HSPC)  
46 (9-12). This receptor is known to be one of the earliest activation markers since its  
47 expression is promptly induced or further upregulated on all studied leukocyte subtypes  
48 upon activation (10). CD69 is highly expressed in leukocytes during infections and at  
49 inflammatory locations in autoimmune and allergic diseases. Galectin-1, S100A8/A9  
50 and myosin light chains 9 and 12 have been proposed as CD69 ligands (13-15). The *in*  
51 *vivo* function of CD69 as a regulator of the immune response has been revealed by the  
52 study of CD69-deficient mice using different murine inflammatory models, including  
53 tumor immunity, infection and autoimmune disease models (16-23). The effects of  
54 treatment with the anti-mouse CD69 2.2 nondepleting antibody (anti-mCD69-2.2)  
55 partially resemble the CD69-deficient phenotypes in tumor, arthritis, and contact  
56 hypersensitivity models (20, 24, 25). Roles for CD69 in leukocyte retention in the  
57 thymus and secondary lymphoid organs have been associated with the cis interaction  
58 between CD69 and Sphingosine-1-Phosphate Receptor 1 (S1P<sub>1</sub>), which downregulates  
59 S1P<sub>1</sub> surface expression and inhibits lymphocyte egress from the thymus and peripheral  
60 lymphoid organs (26). In agreement with the role of CD69 in leukocyte retention in the  
61 bone marrow (BM), our recent published study showed that CD69 deficiency or  
62 targeting with nondepleting anti-CD69 mAbs promotes the egress of hematopoietic  
63 precursor cells from the BM (11). Moreover, anti-CD69 mAb treatment induces the

64 expansion of HSPC dependent on mTOR signaling (11). mTOR, which is of chief  
65 importance in cell metabolism, proliferation and survival, can exist in two distinct  
66 complexes: mTORC1, whose downstream targets are p70S6K and 4E-BP1, and  
67 mTORC2, whose activity is monitored by the downstream phosphorylation of Akt at  
68 Serine 473 (27).

69 CD69 has been shown to be expressed in lung lymphocytes after intranasal VACV  
70 infection proportionally to infection virulence. It is also highly expressed on virus-  
71 specific tissue resident memory T cells of virally infected skin (28, 29) and is important  
72 for the retention in the skin of this population (28). In our preceding study, CD69  
73 deficiency resulted in increased early NK cell-dependent control of the infection (21).  
74 These results are in accordance with those obtained investigating in vivo infections with  
75 deletion mutant virus, where inactivation of N1L VACV gene resulted in an enhanced  
76 NK response and reduced numbers of CD69+ leukocytes (30).

77

78 In the present study, we analyzed the effect of targeting CD69 in the VACV infection  
79 model. Anti-CD69 therapy resulted in increased control of VACV infection, and this  
80 control was associated with increased numbers of IFN $\gamma$ - and TNF $\alpha$ -producing NK cells  
81 and CD4+ and CD8+ T cells reacting in a noncognate fashion. In addition, the  
82 percentages of these cytokine-producing cells were increased, indicating that targeting  
83 CD69 increases the reactivity of these effector cells. We showed that the increase in  
84 leukocyte numbers in the peripheral organs induced by targeting CD69 was mediated by  
85 SIP receptor-dependent mTOR signaling. In agreement with the roles of mTOR in  
86 proliferation and cell survival, we found that these parameters increased upon anti-  
87 CD69 therapy, which contributed to the increased leukocyte counts observed in the long  
88 term. Moreover, we observed a sharp induction of the expression of cytokines, many of  
89 which are important in innate immune responses.

90

91 **RESULTS**

92 **Anti-CD69 mAb treatment enhances protection against VACV infection.**

93 First, we tested whether anti-CD69 pretreatment could enhance the control of VACV  
94 infection. To do this we used a human-CD69 transgenic mouse model that carries a  
95 BAC containing the human CD69 gene locus on the mouse CD69<sup>-/-</sup> background  
96 (huCD69). The mice were treated with two doses of 200 µg of anti-human CD69 mAb  
97 2.8 (anti-huCD69-2.8) separated by one week and i.p infected with 1x10<sup>7</sup> plaque-  
98 forming units (pfu) of VACV 5 days after the last mAb dose. The mice were analyzed  
99 for ovarian viral counts and peripheral leukocyte numbers seven days after infection,  
100 when the primary adaptive response is already taking place (Fig. 1A). The treated mice  
101 controlled VACV infection more efficiently than control mice (Fig. 1B). A decrease and  
102 increase in the total leukocyte counts in the BM and spleen, respectively, were  
103 observed, as well as small increases in the lymph node and blood leukocyte counts (Fig.  
104 1C). The numbers of CD8<sup>+</sup> T cells, macrophages and eosinophils were slightly but  
105 significantly increased (Fig. 1D). The treatment also induced an increase in the number  
106 of CD4<sup>+</sup> T cells producing IFN $\gamma$  and a tendency toward higher numbers of CD4<sup>+</sup> T  
107 cells producing TNF $\alpha$  and CD8<sup>+</sup> T cells producing IFN $\gamma$  (Fig. 1E-F). Thus, treatment  
108 with the anti-huCD69-2.8mAb could affect the primary adaptive response to VACV  
109 infection by increasing the number of activated T cells in the periphery. To assess the  
110 effect of CD69 treatment in a more natural experimental model we used an intranasal  
111 low-dose (10<sup>4</sup> pfu) VACV inoculation and monitored weight overtime. Anti-CD69-  
112 treated mice showed a reduced weight loss relative to their non-treated counterparts  
113 (Figure G-H). The differences were already significant 1 day after infection, maintained  
114 overtime and augmented after seven days, showing that the effects of anti-CD69  
115 treatment are long lasting. Similarly, WT mice treated with the anti-mCD69-2.2 mAb  
116 using the same schedule more efficiently limited infection than control-treated mice.  
117 Moreover, the WT mice had strong increases in leukocyte numbers in the spleen, lymph  
118 nodes and blood, and the numbers of the main splenic lymphocyte subsets, dendritic  
119 cells (DCs) and TNF $\alpha$ - and IFN $\gamma$ -producing CD4<sup>+</sup> T cells were augmented (data not  
120 shown). In summary, targeting human and mouse CD69 resulted in an increased ability  
121 to control VACV infection and increased the accumulation of leukocytes, including  
122 effector lymphocytes, in peripheral sites.

123

124 **Targeting CD69 enhances the innate immune response to VACV infection**

125 To study whether the enhanced antiviral control was in part due to a more efficient early  
126 innate response, we performed the same treatment regimen in huCD69 mice and  
127 analyzed viral titers and leukocyte subsets two days after VACV infection (Fig. 2A), at  
128 which time point the adaptive response to VACV infection had not yet developed. At  
129 this early time point, anti-huCD69-2.8 mAb treated mice already showed slightly lower  
130 ovarian viral titers (Fig. 2B). The numbers of total blood and splenic leukocytes (Fig.  
131 2C) and all splenic subtypes analyzed in the mAb-treated mice were increased  
132 compared to those in control mice (Fig. 2D). Moreover, the treatment induced marked  
133 increases in the numbers of TNF $\alpha$ -producing NK, CD8 $^+$  T and CD4 $^+$  T cells and IFN $\gamma$ -  
134 producing NK and CD4 $^+$  T cells and a tendency toward higher numbers of IFN $\gamma$ -  
135 producing CD8 $^+$  T cells (Fig. 2E-F). In a short-term treatment experiment, this  
136 increased control is already detected in the spleen after 6 hours of infection (Fig. 2G).

137 Very similar results were obtained when WT mice were treated with only one injection  
138 of anti-mCD69-2.2 administered 24 hours before VACV infection and analyzed at 2  
139 days postinfection (Fig. 3A-H). Also, there was a significant difference in ovarian viral  
140 titers when the treatment with anti-mCD69-2.2 was administered 24 h after VACV  
141 exposure (Fig. 3I-J).

142 This early time point postinfection at which the antibody pretreatment affects viral titers  
143 suggests a contribution of the innate immune system. To assess the importance of the  
144 innate immune response against VACV infection in the absence of T and B cells, we  
145 infected Rag2 $^{-/-}$  mice pretreated with anti-mCD69-2.2 mAb with  $1 \times 10^6$  pfu of VACV  
146 and analyzed them two days after infection (Fig. 4A). As in the treated WT and huCD69  
147 mice, the anti-CD69-treated Rag2 $^{-/-}$  mice showed lower ovarian viral titers than control  
148 mice (Fig. 4B) and decreased and increased leukocyte numbers in the bone marrow and  
149 spleen, respectively (Fig. 4C). Consistently, in the spleen, targeting CD69 induced  
150 increases in NK cell, monocyte and neutrophil counts (Fig. 4D). Moreover, we found  
151 that the antibody treatment increased the percentages (Fig. 4E) and numbers (Fig. 4F) of  
152 NK cells producing IFN $\gamma$ - and TNF $\alpha$ - and undergoing degranulation (CD107+).

153 Altogether, these results show that anti-CD69 pretreatment increases the innate immune  
154 control of viral infection accompanied by increases in peripheral innate leukocyte  
155 numbers and cytokine-producing T and NK cell numbers. Unlike CD69 deficiency,  
156 however, targeting CD69 increases the percentages of cytokine-producing T and NK

157 cells and degranulating NK cells, suggesting that targeting CD69 augments T and NK  
158 cell reactivity.

159

160 **In the absence of infection, targeting CD69 promotes the proliferation and survival**  
161 **of leukocytes.**

162 Next, we studied whether the differences observed in the infection setting are due to the  
163 effects of the mAb treatment on components of the immune system that will later  
164 respond to the infection. Thus, we were interested in analyzing the effects of the anti-  
165 CD69 mAb treatment schedule in the absence of infection. To study this possibility, we  
166 injected huCD69 mice with two doses of 200 $\mu$ g of anti-huCD69 2.8 separated by one  
167 week and analyzed the BM and splenic numbers of leukocyte subtypes 5 days after the  
168 second dose. Total leukocyte counts were decreased in the BM and increased in the  
169 secondary lymphoid organs of the treated mice (Fig. 5A). The numbers of NK cells, T  
170 cells and B cells were augmented in the spleen (Fig. 5B). Then, we studied whether  
171 mechanisms such as increased leukocyte proliferation and/or survival might contribute  
172 to the increased peripheral cellularity observed in the longer term. Thus, we tested the  
173 effect of anti-huCD69 2.8 treatment on leukocyte proliferation. HuCD69 mice were  
174 administered the anti-huCD69 2.8 mAb, and after 24 hours, they were injected with  
175 bromodeoxyuridine (BrdU) and analyzed 3 hours later. BrdU incorporation was  
176 increased in most of the major leukocyte lineages in the BM and spleen (Fig. 6A-B). Of  
177 note, after only a 3-hour pulse, the BrdU<sup>+</sup> myeloid cells likely consisted mainly of  
178 differentiated myeloid cells, which have been demonstrated to be able to proliferate *in*  
179 *vivo* (31-34).

180 For cell survival analysis, since dead cells are quickly phagocytized *in vivo*, we  
181 performed *ex vivo* cultures of splenocytes from anti-human CD69 2.8-treated mice and  
182 analyzed the spontaneous cell death by propidium iodide (PI) staining at different times  
183 of culture. Significant differences were found at early time points, and these differences  
184 increased over time (Fig. 6C). Altogether, these data suggest that anti-CD69 mAb  
185 treatment may achieve greater peripheral cellularity through increased survival and  
186 proliferation of mature leukocytes and that this state can be maintained by repeated anti-  
187 CD69 mAb administration.

188

189 **Targeting CD69 promotes mitogenic and proinflammatory cytokine production**

190 We previously described that the anti-mCD69-2.2 mAb induces T cell proliferation  
191 through IL-2 production by plasmacytoid DCs and interleukin-2 receptor alpha (IL-  
192 2Ra) expression upregulation in memory T cells (9). Thus, we tested whether anti-  
193 human CD69 2.8 treatment could also upregulate IL-2 and IL-2Ra expression. As  
194 expected, we found increased intracellular IL-2 and surface IL-2Ra levels in cells from  
195 the bone marrow, spleen and blood 24 h after anti-huCD69 2.8 treatment (Fig. 7A).  
196 These increases may contribute to the higher T and NK cell proliferation observed in  
197 anti-CD69-treated mice.

198 Previous studies performed in our laboratory showed decreased transforming growth  
199 factor beta (TGF- $\beta$ ) and increased proinflammatory cytokine expression in CD69<sup>-/-</sup>  
200 mice, which was related to increased splenic cellularity and decreased spontaneous cell  
201 death. We wanted to test whether this could also be achieved by targeting CD69 with a  
202 mAb. Thus, we assessed the expression of TGF- $\beta$  and several proinflammatory  
203 cytokines (IL-1 $\alpha$  and  $\beta$ ; LT $\alpha$  and  $\beta$ ; IL-17 $\alpha$ ,  $\beta$  and f; IL-21; IFN $\gamma$ ; and TNF $\alpha$ ) and  
204 chemokines (CCL2 and CCL12) 24 h after anti-huCD69 2.8 treatment by real-time PCR  
205 (RT-PCR). We found a decrease in TGF- $\beta$  expression in the spleen of treated mice (Fig.  
206 7B). Instead, the splenic messenger RNA (mRNA) levels of IL-1 $\alpha$  and  $\beta$ , LT $\alpha$  and  $\beta$ ,  
207 IL-17 $\beta$  and f, IL-21, IFN $\gamma$ , TNF $\alpha$ , CCL2 and CCL12 were increased (Fig. 7D-G). We  
208 also measured the expression of IL-1 $\alpha$  and  $\beta$ , IL-21, IL-17 f, IFN $\gamma$ , IL-3 and IL-6 at the  
209 protein level in supernatants of huCD69 splenocytes 1 day after anti-huCD69 mAb 2.8  
210 treatment with a Luminex assay. The results showed highly significant increases in IL-  
211 1 $\alpha$ , IL-1 $\beta$ , IFN $\gamma$  and IL-6 production (Fig. 7C) in the anti-CD69 mAb 2.8-treated mice.  
212 In summary, targeting CD69 rapidly induces a promitogenic and proinflammatory  
213 cytokine profile.

214

215 **Targeting CD69 induces leukocyte accumulation in the spleen through mTOR**  
216 **signaling.**

217 We reported that anti-CD69 mAb-induced BM mobilization is dependent on S1P  
218 receptor function since this migration is inhibited by S1P receptor desensitization with  
219 fingolimod (FTY720) treatment (11).

220 Several reports have shown that S1P mediates BM mobilization through mTOR (35-37).  
221 We showed that mTOR inhibition in huCD69 mice by rapamycin pretreatment blocked  
222 the increase in splenic cellularity and partially inhibited the decrease in whole BM cell  
223 numbers induced by the anti-hCD69 mAb 2.8 at 24 h posttreatment (Fig. 8A),  
224 suggesting that mTOR also mediates the accumulation of leukocytes in the spleen  
225 induced by targeting CD69. Consistently, anti-CD69 mAb 2.8 treatment induced the  
226 phosphorylation of the mTOR target p70S6K, and this effect was inhibited in the spleen  
227 by rapamycin treatment (Fig. 8B). Moreover, FTY720 treatment also inhibited the  
228 phosphorylation of p70S6K in the spleen (Fig. 8C), suggesting that targeting CD69  
229 induces mTOR signaling through S1P receptors. Altogether, the presented data suggest  
230 that the effect on leukocyte accumulation in the spleen induced by targeting CD69 is  
231 mediated by S1P receptor signaling through the mTORC1 cascade.

## 232 **DISCUSSION**

233 In the present study, we show that anti-CD69 mAb pretreatment enhances innate  
234 immune protection against VACV infection related to enhanced numbers of peripheral  
235 cellular effectors, which can be explained by increased BM cell output and leukocyte  
236 proliferation and survival. Although they rely on the murine immune system, the use of  
237 huCD69 mice allows to show that the interaction of the anti-human CD69-2.8 mAb  
238 with the human CD69 molecule is such that, like the treatment of WT mice with anti-  
239 mouse-2.2, will also induce innate immune activation and protection in front of viral  
240 infection *in vivo*. Human and mouse CD69 have more than 70% of conserved residues.  
241 The comparable effects of anti-human and anti-mouse CD69 targeting suggest that  
242 conserved motifs allow the human CD69 molecule to act like the mouse CD69 in the  
243 context of murine immune system in the CD69<sup>-/-</sup> background.

244 In previous reports, targeting CD69 resulted in outcomes similar to those seen with  
245 CD69 deficiency in several murine models of cancer and autoimmune disease (22, 24,  
246 25). Similar outcomes are also seen in the VACV infection model since, like targeting  
247 CD69, CD69 deficiency also enhances the host innate immune resistance to VACV  
248 infection accompanied by increases in peripheral cellularity and the numbers of T and  
249 NK cells producing IFN $\gamma$  and TNF $\alpha$  and degranulating NK cells (21). The similarities in  
250 cellularity and immune control in early VACV infection between targeting CD69 and  
251 CD69 deficiency could be due to targeting CD69 simulating the avoidance of the cis  
252 interaction between CD69 and S1P1 and the downregulation of S1P1 expression, which  
253 hinders BM cell egress, seen in CD69 deficiency. However, several data points indicate  
254 that the mechanisms underlying the effects of targeting CD69 and CD69 deficiency may  
255 differ to some extent.

256 On the one hand, although both settings show increases in the numbers of cytokine-  
257 producing T and NK cells, only targeting CD69 shows an increase in the percentages of  
258 these cells. For NK cells, this finding suggests that, unlike CD69 deficiency, targeting  
259 CD69 enhances NK cell reactivity, probably through cytokine-mediated NK cell  
260 priming. The T cells producing IFN $\gamma$  and TNF $\alpha$  upon restimulation at two days  
261 postinfection are likely T cells activated in a noncognate fashion by cytokines. This  
262 result may support the conclusion that targeting CD69 but not CD69 deficiency induces  
263 proinflammatory cytokine production per se. At seven days postinfection, the detected

264 IFN $\gamma$ <sup>+</sup> and TNF $\alpha$ <sup>+</sup> T cells may include VACV-specific T cells. However, we do not  
265 expect that specific T cells account for the differences, since anti-mCD69-2.2 mAb  
266 treatment *in vivo* did not affect the frequency of splenic VACV-specific T cells 1 week  
267 after intraperitoneal VACV inoculation (38). Instead, in a model of local virus  
268 infection of the skin, CD69 enhanced the retention of specific resident memory T cells  
269 in the infected skin already at week 1 post-infection, but not in the spleen (28). The  
270 differences may be attributed to the CD69 function in the retention of memory T cells in  
271 tissue and non in lymphoid organs.

272 Another difference between CD69 deficiency and targeting CD69 is that while targeting  
273 CD69 augments the leukocyte proliferation rate, CD69 deficiency has no effect on that  
274 rate (21, 38). This result also argues against the presence of increased amounts of  
275 mitogenic cytokines in CD69 knockout (KO) mice under steady-state conditions,  
276 although CD69 KO mice do show proinflammatory cytokine profiles upon the induction  
277 of cancer or autoimmune disease (18, 25).

278 In both CD69-deficient mice and CD69-targeted mice, cell survival is increased (21).  
279 This result may be related to the fact that TGF $\beta$  expression is decreased in almost all  
280 disease models performed with both CD69<sup>-/-</sup> and anti-CD69 mAb-treated mice (18, 22-  
281 25, 39, 40). TGF- $\beta$  is a pleiotropic cytokine, and one of its reported functions is the  
282 control of cell survival, including the survival of leukocytes (41). Interestingly, CD69  
283 deficiency in FoxP3 Tregs leads to decreased TGF $\beta$  production, and both CD69  
284 deficiency and targeting CD69 in these cells hinder their suppressive function (39).

285 Another observation indicates that the situations in CD69-targeted and CD69-deficient  
286 mice differ; in CD69-targeted mice, there is massive egress of cells with undetectable  
287 CD69 surface levels, such as neutrophils, which suggests the contribution of a cell  
288 extrinsic mechanism, putatively mediated by soluble mediators. One of these soluble  
289 mediators is likely to be S1P acting through mTOR signaling since S1P receptor  
290 desensitization with FTY720 inhibits anti-CD69 treatment-induced egress from the BM  
291 (11) and mTOR signaling, and mTOR inhibition with rapamycin partly inhibits BM  
292 mobilization. Other possible soluble mediators are cytokines and chemokines. In the  
293 present work, we observed enhanced expression of several innate cytokines and  
294 chemokines. Some of these cytokines, i.e., IL-1, IL-2 and IFN $\gamma$ , activate mTOR through  
295 PI3K and phospho-Akt T308. Growth factors can also activate mTOR through ERK1/2

296 signaling (42). Instead, S1P activates mTORC1 through the E3-ubiquitin ligase PAM in  
297 a manner independent of PI3K, Akt and ERK1/2 (43). The fact that we did not detect  
298 any phosphorylation of Akt T308 or ERK1/2 may suggest that, at the time of analysis,  
299 targeting CD69 had induced mTORC1 activation mainly through S1P receptors rather  
300 than through cytokines or growth factors.

301 CD69 has been described to negatively regulates Th17 cell differentiation through the  
302 immunoregulatory molecule Galectin 1(15) and to promote Treg differentiation thorough  
303 interaction with the complex S100A8/S100A9 (14). The antibody could be disrupting  
304 the interactions with these trans ligands and thus inducing immune activation.  
305 Moreover, the antibody could be affecting CD69 interaction with its ligands in cis S1P1  
306 and CD69 downregulation of surface S1P1 may be hindered by mAb binding. This,  
307 together with that sustained S1P1 surface expression enhances mTOR activation on T  
308 cells (44) may contribute to anti-CD69-induced mTOR activation. VACV employs  
309 numerous immune evasion mechanisms to decoy, inhibit the production, and block the  
310 signaling of type I and II IFNs, TNF $\alpha$ , IL-1 and IL-18, which amplify the innate  
311 immune response, influence the adaptive response to the virus and, in the case of type I  
312 and II IFNs and TNF $\alpha$ , have direct antiviral activity (45). Thus, the observed augmented  
313 expression of IFN $\gamma$ , TNF $\alpha$  and IL-1 as well as the possible augmentation of the  
314 expression of other cytokines may counteract these immune evasion mechanisms of the  
315 virus. Instead, an enhanced proinflammatory cytokine response is detrimental in the  
316 cases of other pathogens.

317 The data presented here showing that targeting CD69 enhances the early control of  
318 pathogens encourage future testing of anti-CD69 mAbs as agents for enhancing the  
319 immune responses in vaccine-mediated protection and against infection in leukopenia  
320 treatment.

## 321 **Materials and methods**

### 322 **Mice and *in vivo* protocols**

323 All mice used were males or females between 6 and 12 weeks of age that were bred and  
324 housed under specific pathogen-free conditions in the *Instituto de Salud Carlos III*  
325 (*ISCIII*) animal facilities (Madrid). HuCD69 mice were obtained by transgenesis of a  
326 human CD69 BAC containing 100 kb of the CD69 gene, which was generated by  
327 Bristol Myers and kindly provided by Dr. Robert Graziano. These mice are in the  
328 mouse CD69<sup>-/-</sup> background and carry three copies of the human CD69 BAC, which  
329 were maintained in hemizygoty. Since the human CD69 BAC contains the entire  
330 human CD69 gene locus (around 100kb), where CD69 transcription is driven by the  
331 original regulatory regions, these mice express human CD69 in a regulated fashion, as  
332 previously shown (24). Rag2<sup>-/-</sup> in Balb/c genetic background and C57BL6 mice were  
333 also used.

334 Mice treated with FTY720 (Sigma-Aldrich) were injected intraperitoneally (i.p) with  
335 two doses of FTY720 (5 mg/kg) separated by 24 hours.

336 The mice that received rapamycin (Selleckchem) were treated with 480 mg of  
337 rapamycin/kg administered i.p for five days.

338 In proliferation assays, mice were injected intraperitoneally with 1 mg of BrdU and after  
339 three hours, splenocytes and BM cells were collected. BrdU staining was performed  
340 using a BrdU Flow kit (Beckton Dickinson) and an anti-mouse BrdU antibody (clone  
341 B44) according to the manufacturer's instructions.

### 342 **Antibodies and cell culture**

343 The anti-huCD69-2.8 mAb and anti-mCD69-2.2 mAb, both of the IgG1 isotype, bind to  
344 the human and the mouse CD69 molecule respectively. They were generated in our  
345 laboratory (24). Neither of them activates the complement system or induces ADCC, as  
346 previously experimentally demonstrated (24). Since anti-huCD69-2.8 mAb does not  
347 cross-react with mouse CD69 and anti-mCD69-2.2 mAb does not cross-react with  
348 human CD69, we used the anti-mouse-CD69-2.2 mAb as isotype control of anti-human-  
349 CD69 mAb experiments and *vice versa*. The mAbs were purified from concentrated  
350 hybridoma supernatants using protein G columns (GE Healthcare, Piscataway, NJ,  
351 USA), further purified by Zeba Spin desalting columns (*Thermo Scientific*) and stored at

352 -80°C. The purified mAbs were tested with CD69<sup>-/-</sup> BM-derived DC (BMDC) cultures  
353 at a concentration of 10 µg/ml, and were unable to upregulate CD80 or CD86  
354 expression in these cultures. HuCD69 mice were intravenously treated with one dose of  
355 500 µg of anti-huCD69 2.8 or with two doses of 200 µg of anti-huCD69 2.8 separated  
356 by a week, and 5 days after the second dose, the mice were analyzed or infected as  
357 appropriate for the experiment. In repeated experiments, we injected control mice with  
358 isotype control mAb in the first experiment, and PBS when the experiment was  
359 repeated, obtaining comparable results. CD69<sup>+/+</sup> and Rag2<sup>-/-</sup> mice were treated  
360 following a protocol similar to that used for the HuCD69 mice but with the anti-  
361 mCD69-2.2 mAb administered i.v. and the anti-huCD69-2.8 mAb or PBS used as a  
362 control.

### 363 **Cell Isolation**

364 Bone marrow was collected from the two femurs of each mouse. Blood was collected  
365 by intracardiac puncture and diluted in 10 ml of 2 mM EDTA PBS, and the numbers  
366 shown are the white blood cell counts per 1 ml of blood. The thymus and spleen were  
367 disaggregated, and the cells were washed in PBS. Erythrocytes were lysed with an  
368 ammonium chloride potassium (ACK) solution in all samples, and leukocytes were  
369 labeled and analyzed by flow cytometry.

### 370 **Abs and flow cytometry**

371 Cells from the bone marrow, spleen, blood, thymus and lymph nodes were incubated  
372 with anti-CD16/32 (Fc-block 2.4G2; BD Biosciences, Franklin Lakes, NJ, USA). The  
373 following antibodies against mouse intracellular and surface antigens were purchased  
374 from eBioscience (San Diego, CA): anti-CD4 (clone RM4-5), anti-CD8 (clone 53-6.7 or  
375 clone Ly-2), anti-CD11b (clone M1/70), anti-CD11c (clone N418 or clone HL3), anti-  
376 CD19 (clone eBio1D3), anti-CD49b (clone DX5), anti-CD69 (clone H1.2F3), anti-  
377 CD107a (clone eBio4A3), anti-CD117 (clone 2B8), anti-F480 (clone BM8), anti-GR1  
378 (clone RB6-8C5), anti-IFN-γ (clone XMG 1.2), anti-NKp46 (clone 29A1.4), anti-CD3  
379 (clone 17A2), anti-IL2 (clone JES6-5H4), anti-CD25 (clone 3C7), and anti-TNF-α  
380 (clone MP6-XT22). Cells were analyzed with a FACSCanto flow cytometer (Becton  
381 Dickinson, Franklin Lakes, NJ, USA) using BD FACSDiva software (Becton  
382 Dickinson), and data were analyzed with FlowJo (TreeStar Inc., Ashland, OR, USA).

383 To assess the intracellular production of IFN- $\gamma$ , TNF- $\alpha$  and IL-2,  $2 \times 10^6$  splenocytes  
384 were incubated in the presence of brefeldin A (BFA) (5  $\mu\text{g/ml}$ ) for 4 h at 37°C and  
385 washed. Alternatively, cells were restimulated with 10 ng/ml PMA (*Phorbol 12-*  
386 *myristate 13-acetate*) and 1  $\mu\text{g/ml}$  ionomycin or RPMI medium only in the presence of  
387 BFA (5  $\mu\text{g/ml}$ ) for 4 hours at 37°C. Following incubation, the cells were fixed with 4%  
388 paraformaldehyde (Electron Microscopy Sciences) for 12 minutes at room temperature  
389 in the dark and permeabilized with 1% saponin (Sigma-Aldrich) in 1x PBS and 3% fetal  
390 bovine serum (FBS) for 20 min at 4°C. The cells were acquired with a FACSCanto  
391 instrument (Becton Dickinson, Franklin Lakes, NJ, and USA) using BD FACSDiva  
392 software (Becton Dickinson), and the data were analyzed with FlowJo (TreeStar Inc.,  
393 Ashland, OR, USA).

#### 394 **Vaccinia virus**

395 The Western Reserve strain of VACV (provided by Dr. Daniel Lopez) was grown in  
396 African green monkey kidney fibroblast cells (CV1 cells, provided by Dr. Daniel  
397 Lopez) cultured in D-MEM supplemented with 10% FBS, 2 mM L-glutamine, 100  
398 U/mL penicillin, 100  $\mu\text{g/mL}$  streptomycin and 5  $\mu\text{M}$   $\beta$ -mercaptoethanol. The titer was  
399 determined by a plaque assay using CV1 cells, and the viral stock was stored at -80°C in  
400 PBS until use. A total of  $1 \times 10^6$  pfu was injected into Rag2<sup>-/-</sup> mice, and  $1 \times 10^7$  pfu was  
401 injected intraperitoneally into immunocompetent mice in 0.2 ml of PBS. The viral load  
402 was measured by a plaque-forming assay. In brief, female mice were sacrificed at the  
403 indicated times, and the ovaries were harvested and stored at -80°C in 0.5 ml of PBS  
404 until use. The ovaries from individual mice were first homogenized and subjected to  
405 three freeze-thaw cycles. Serial dilutions were plated on confluent CV1 cells. After one  
406 day of culture at 37°C, plates were stained with crystal violet, and the plaques were  
407 counted.

#### 408 **Luminex assay**

409 Splenocytes were collected from HuCD69 mice 24 hours after treatment with the anti-  
410 huCD692.8 mAb or no treatment in 1 ml of RPMI medium supplemented with 10%  
411 FBS, 2 mM L-glutamine, 100 U/mL penicillin, 100  $\mu\text{g/mL}$  streptomycin and 5  $\mu\text{M}$   $\beta$ -  
412 mercaptoethanol. Supernatants were obtained after centrifugation. The levels of IFN- $\gamma$ ,  
413 IL-1 $\alpha$ , IL-1 $\beta$ , IL-17f, IL-21, IL-3 and IL-6 were determined by using ProcartaPlex  
414 custom assays (Affymetrix) and Luminex.

415 **Gene expression analysis**

416 The expression of inflammatory genes was evaluated with the Mouse RT<sup>2</sup>*Profiler* PCR  
417 Inflammatory Cytokines and Receptors Array (SABiosciences). Ribonucleic acid  
418 (RNA) was obtained from the spleen of mice treated with the anti-huCD69-2.8 mAb or  
419 untreated mice using the RNeasy Mini Kit, and a First Standard kit (SABiosciences)  
420 was used for cDNA synthesis. The RT<sup>2</sup>*Profiler* array was probed according to the  
421 manufacturer's protocol using the Profiler PCR Array System and SYBR  
422 Green/Fluorescein qPCR Master Mix (SABiosciences) with an ABI 7500 Fast sequence  
423 analyzer (Applied Biosystems). Gene expression was measured with a web-based  
424 software package for the PCR Array System  
425 (<http://www.superarray.com/pcr/arrayanalysis.php>), which automatically performs all  
426  $\Delta\Delta\text{Ct}$ -based fold-change calculations from the specific uploaded raw threshold cycle  
427 data.

428 For qPCR assays, RNA was treated with RQ1 RNase-Free DNase (Promega) prior to  
429 cDNA synthesis from 5  $\mu\text{g}$  of total RNA with GoScript™ Reverse Transcriptase  
430 (Promega) using a combination of random primers and oligo dT. The cDNA samples  
431 were diluted to 50 ng/ $\mu\text{l}$ . Real-time PCR with SYBR green detection was performed  
432 with 1  $\mu\text{l}$  of cDNA.. Expression was calculated by the formula  $2^{-\Delta\text{Ct}}$ , using  $\beta$ -actin to  
433 normalize sample loading. The primer sets used for qPCR are listed below.

434 **IL1- $\alpha$  Forward:** acgtcaagcaacgggaagat

435 **IL1- $\alpha$  Reverse:** aaggtgctgatctgggttg

436 **IL1- $\beta$  Forward:** aatgaaagacggcacacca

437 **IL1- $\beta$  Reverse:** accgttttccatcttcttttg

438 **TNF- $\alpha$  Forward:**gcctcttctcattcctgcttg

439 **TNF- $\alpha$  Reverse:** ctgatgagaggaggccatt

440 **IL-17F Forward:**gcatttctgtcccacgtgaa

441 **IL-17F Reverse:** tgggggtctcgagtgatg

442 **IL-21 Forward:** cgctcctgattagacttcgt

443 **IL-21 Reverse:** tgctcacagtgccctttac

444 **CCL2 Forward:** caggtccctgcatgcttct

445 **CCL2 Reverse:** gtggggcgtaactgcatct

446 **CCL12 Forward:** gaatcacaagcagccagtgtc

447 **CCL12 Reverse:** ttctcctggggtcagcaca

448 **β-ACTIN Forward:** actgtcgagtcgcgtcca

449 **β-ACTIN Reverse:** tcatccatggcgaactggtg

#### 450 **Cell death assay**

451 Splenocytes from noninfected mice were cultured in 24-well plates ( $1 \times 10^6$  cells/ml),  
452 and cell death was assayed at different times during the culture by staining with PI,  
453 followed by flow cytometric analysis.

#### 454 **Biochemical Analysis**

455 Collected cells from the BM and spleen were lysed using Triton lysis buffer (20 mM  
456 Tris [pH 7.4], 1% Triton X-100, 10% glycerol, 137 mM NaCl, 2 mM EDTA, 25 mM β-  
457 glycerophosphate, 1 mM sodium orthovanadate, 1 mM phenylmethylsulfonyl fluoride,  
458 and 10 μg/ml aprotinin and leupeptin). Extracts (30 μg of protein) were examined by  
459 protein immunoblot analysis with antibodies against phospho-(Thr389)-p70S6K,  
460 p70S6K, phospho-(Ser240/244)-S6, S6, phospho-(Ser2448)-mTOR, and mTOR, all of  
461 which were obtained from Cell Signaling, and antibodies against GAPDH (Santa Cruz  
462 Biotechnology Inc.) or vinculin (Sigma).

#### 463 **Ethics Statement**

464 All procedures involving animals and their care were approved by the *ISCIII* Ethics  
465 Committees (OEBA M-05-2015) and the Comunidad de Madrid (PROEX 156/15) and  
466 followed the current Spanish legislation (Real Decreto 53/2013), which are in  
467 compliance with European laws (Directive 2010/63/EU).

#### 468 **Statistical analysis**

469 All data were plotted and statistically analyzed using GraphPad Prism software. Graphs  
470 show means and standard errors of the mean (SEM). Statistical significance was

471 determined using an unpaired two-tailed *t*-test (\*  $p < 0.05$ , \*\*  $p < 0.01$ , \*\*\*  $p < 0.005$ ).  
472  $p < 0.05$  was considered significant

#### 473 **Author contributions**

474 LN, JR and ML performed the experiments. LN, GS and PL designed the experiments.  
475 AA provided technical support. LN, EAP, GS and DL discussed the data. LN, EAP and  
476 PL wrote the manuscript. PL was responsible for the project design and management.

#### 477 **Acknowledgments**

478 We thank Daniel Baizan, Cristina Pintos and Maria Clemente for performing the mouse  
479 husbandry.

#### 480 **Conflict of interests**

481 No competing interests declared.

#### 482 **Funding**

483 The study was supported by the Instituto de Salud Carlos III MPY 1366/13 and MPY  
484 1346/16. M L was supported by SAF2015-74112-JIN from MINECO. G S was  
485 supported by ERC 260464, EFSO 2030, MINECO-FEDER SAF2016-79126-R and  
486 Comunidad de Madrid S2010/BMD-2326. The CNIC is supported by the Ministerio de  
487 Economía y Competitividad and the Pro-CNIC Foundation. The Pro-CNIC Foundation  
488 is a Severo Ochoa Center of Excellence (MINECO award SEV-2015-0505).

489  
490  
491  
492  
493  
494  
495  
496  
497  
498  
499  
500  
501  
502  
503  
504  
505  
506  
507  
508  
509  
510  
511  
512  
513  
514  
515  
516  
517  
518  
519  
520  
521  
522  
523  
524  
525  
526  
527  
528  
529  
530  
531  
532  
533  
534  
535  
536  
537  
538  
539  
540

## References

1. Martinez J, Huang X, Yang Y. 2008. Direct action of type I IFN on NK cells is required for their activation in response to vaccinia viral infection in vivo. *J Immunol* 180:1592-7.
2. Xu R, Johnson AJ, Liggitt D, Bevan MJ. 2004. Cellular and humoral immunity against vaccinia virus infection of mice. *J Immunol* 172:6265-71.
3. Garcia F, Bernaldo de Quiros JC, Gomez CE, Perdiguero B, Najera JL, Jimenez V, Garcia-Arriaza J, Guardo AC, Perez I, Diaz-Brito V, Conde MS, Gonzalez N, Alvarez A, Alcami J, Jimenez JL, Pich J, Arnaiz JA, Maleno MJ, Leon A, Munoz-Fernandez MA, Liljestrom P, Weber J, Pantaleo G, Gatell JM, Plana M, Esteban M. 2011. Safety and immunogenicity of a modified pox vector-based HIV/AIDS vaccine candidate expressing Env, Gag, Pol and Nef proteins of HIV-1 subtype B (MVA-B) in healthy HIV-1-uninfected volunteers: A phase I clinical trial (RISVAC02). *Vaccine* 29:8309-16.
4. Cavanaugh JS, Awi D, Mendy M, Hill AV, Whittle H, McConkey SJ. 2011. Partially randomized, non-blinded trial of DNA and MVA therapeutic vaccines based on hepatitis B virus surface protein for chronic HBV infection. *PLoS One* 6:e14626.
5. Berthoud TK, Hamill M, Lillie PJ, Hwenda L, Collins KA, Ewer KJ, Milicic A, Poyntz HC, Lambe T, Fletcher HA, Hill AV, Gilbert SC. 2011. Potent CD8+ T-cell immunogenicity in humans of a novel heterosubtypic influenza A vaccine, MVA-NP+M1. *Clin Infect Dis* 52:1-7.
6. Langford CJ, Edwards SJ, Smith GL, Mitchell GF, Moss B, Kemp DJ, Anders RF. 1986. Anchoring a secreted plasmodium antigen on the surface of recombinant vaccinia virus-infected cells increases its immunogenicity. *Mol Cell Biol* 6:3191-9.
7. Bejon P, Ogada E, Mwangi T, Milligan P, Lang T, Fegan G, Gilbert SC, Peshu N, Marsh K, Hill AV. 2007. Extended follow-up following a phase 2b randomized trial of the candidate malaria vaccines FP9 ME-TRAP and MVA ME-TRAP among children in Kenya. *PLoS One* 2:e707.
8. Wakamiya N, Wang YL, Imai H, Gu HX, Ueda S, Kato S. 1986. Feasibility of UV-inactivated vaccinia virus in the modification of tumor cells for augmentation of their immunogenicity. *Cancer Immunol Immunother* 23:125-9.
9. Alari-Pahissa E, Vega-Ramos J, Zhang JG, Castano AR, Turley SJ, Villadangos JA, Lauzurica P. 2012. Differential effect of CD69 targeting on bystander and antigen-specific T cell proliferation. *J Leukoc Biol* 92:145-58.
10. Sancho D, Gomez M, Sanchez-Madrid F. 2005. CD69 is an immunoregulatory molecule induced following activation. *Trends Immunol* 26:136-40.
11. Notario L, Alari-Pahissa E, Albentosa A, Leiva M, Sabio G, Lauzurica P. 2018. Anti-CD69 therapy induces rapid mobilization and high proliferation of HSPCs through S1P and mTOR. *Leukemia* doi:10.1038/s41375-018-0052-x.
12. Tassone P, Turco MC, Tuccillo F, Bonelli P, Morrone G, Cecco L, Cerra M, Bond H, Di Nicola M, Gianni AM, Venuta S. 1996. CD69 expression on primitive progenitor cells and hematopoietic malignancies. *Tissue Antigens* 48:65-8.
13. Hayashizaki K, Kimura MY, Tokoyoda K, Hosokawa H, Shinoda K, Hirahara K, Ichikawa T, Onodera A, Hanazawa A, Iwamura C, Kakuta J, Muramoto K, Motohashi S, Tumes DJ, Iinuma T, Yamamoto H, Ikehara Y, Okamoto Y, Nakayama T. 2016. Myosin light chains 9 and 12 are functional ligands for CD69 that regulate airway inflammation. *Sci Immunol* 1:eaaf9154.
14. Lin CR, Wei TY, Tsai HY, Wu YT, Wu PY, Chen ST. 2015. Glycosylation-dependent interaction between CD69 and S100A8/S100A9 complex is required for regulatory T-cell differentiation. *FASEB J* 29:5006-17.
15. de la Fuente H, Cruz-Adalia A, Martinez Del Hoyo G, Cibrian-Vera D, Bonay P, Perez-Hernandez D, Vazquez J, Navarro P, Gutierrez-Gallego R, Ramirez-Huesca M, Martin P, Sanchez-Madrid F. 2014. The leukocyte activation receptor CD69 controls T cell differentiation through its interaction with galectin-1. *Mol Cell Biol* 34:2479-87.

- 541 16. Cibrian D, Sanchez-Madrid F. 2017. CD69: from activation marker to metabolic  
542 gatekeeper. *Eur J Immunol* 47:946-953.
- 543 17. Cruz-Adalia A, Jimenez-Borreguero LJ, Ramirez-Huesca M, Chico-Calero I, Barreiro O,  
544 Lopez-Conesa E, Fresno M, Sanchez-Madrid F, Martin P. 2010. CD69 limits the severity  
545 of cardiomyopathy after autoimmune myocarditis. *Circulation* 122:1396-404.
- 546 18. Esplugues E, Sancho D, Vega-Ramos J, Martinez C, Syrbe U, Hamann A, Engel P,  
547 Sanchez-Madrid F, Lauzurica P. 2003. Enhanced antitumor immunity in mice deficient  
548 in CD69. *J Exp Med* 197:1093-106.
- 549 19. Gomez M, Sanz-Gonzalez SM, Abu Nabah YN, Lamana A, Sanchez-Madrid F, Andres V.  
550 2009. Atherosclerosis development in apolipoprotein E-null mice deficient for CD69.  
551 *Cardiovasc Res* 81:197-205.
- 552 20. Martin P, Gomez M, Lamana A, Matesanz Marin A, Cortes JR, Ramirez-Huesca M,  
553 Barreiro O, Lopez-Romero P, Gutierrez-Vazquez C, de la Fuente H, Cruz-Adalia A,  
554 Sanchez-Madrid F. 2010. The leukocyte activation antigen CD69 limits allergic asthma  
555 and skin contact hypersensitivity. *J Allergy Clin Immunol* 126:355-65, 365 e1-3.
- 556 21. Notario L, Alari-Pahissa E, de Molina A, Lauzurica P. 2016. CD69 Deficiency Enhances  
557 the Host Response to Vaccinia Virus Infection through Altered NK Cell Homeostasis. *J*  
558 *Virology* 90:6464-6474.
- 559 22. Sancho D, Gomez M, Viedma F, Esplugues E, Gordon-Alonso M, Garcia-Lopez MA, de la  
560 Fuente H, Martinez AC, Lauzurica P, Sanchez-Madrid F. 2003. CD69 downregulates  
561 autoimmune reactivity through active transforming growth factor-beta production in  
562 collagen-induced arthritis. *J Clin Invest* 112:872-82.
- 563 23. Vega-Ramos J, Alari-Pahissa E, Valle JD, Carrasco-Marin E, Esplugues E, Borrás M,  
564 Martinez AC, Lauzurica P. 2010. CD69 limits early inflammatory diseases associated  
565 with immune response to *Listeria monocytogenes* infection. *Immunol Cell Biol* 88:707-  
566 15.
- 567 24. Esplugues E, Vega-Ramos J, Cartoixa D, Vazquez BN, Salaet I, Engel P, Lauzurica P.  
568 2005. Induction of tumor NK-cell immunity by anti-CD69 antibody therapy. *Blood*  
569 105:4399-406.
- 570 25. Sancho D, Gomez M, Martinez Del Hoyo G, Lamana A, Esplugues E, Lauzurica P,  
571 Martinez AC, Sanchez-Madrid F. 2006. CD69 targeting differentially affects the course  
572 of collagen-induced arthritis. *J Leukoc Biol* 80:1233-41.
- 573 26. Matloubian M, Lo CG, Cinamon G, Lesneski MJ, Xu Y, Brinkmann V, Allende ML, Proia  
574 RL, Cyster JG. 2004. Lymphocyte egress from thymus and peripheral lymphoid organs  
575 is dependent on S1P receptor 1. *Nature* 427:355-60.
- 576 27. Zoncu R, Efeyan A, Sabatini DM. 2011. mTOR: from growth signal integration to cancer,  
577 diabetes and ageing. *Nat Rev Mol Cell Biol* 12:21-35.
- 578 28. Mackay LK, Rahimpour A, Ma JZ, Collins N, Stock AT, Hafon ML, Vega-Ramos J,  
579 Lauzurica P, Mueller SN, Stefanovic T, Tschärke DC, Heath WR, Inouye M, Carbone FR,  
580 Gebhardt T. 2013. The developmental pathway for CD103(+)CD8+ tissue-resident  
581 memory T cells of skin. *Nat Immunol* 14:1294-301.
- 582 29. Khan TN, Mooster JL, Kilgore AM, Osborn JF, Nolz JC. 2016. Local antigen in  
583 nonlymphoid tissue promotes resident memory CD8+ T cell formation during viral  
584 infection. *J Exp Med* 213:951-66.
- 585 30. Jacobs N, Bartlett NW, Clark RH, Smith GL. 2008. Vaccinia virus lacking the Bcl-2-like  
586 protein N1 induces a stronger natural killer cell response to infection. *J Gen Virol*  
587 89:2877-81.
- 588 31. Jenkins SJ, Ruckerl D, Cook PC, Jones LH, Finkelman FD, van Rooijen N, MacDonald AS,  
589 Allen JE. 2011. Local macrophage proliferation, rather than recruitment from the  
590 blood, is a signature of TH2 inflammation. *Science* 332:1284-8.
- 591 32. Robbins CS, Hilgendorf I, Weber GF, Theurl I, Iwamoto Y, Figueiredo JL, Gorbátov R,  
592 Sukhova GK, Gerhardt LM, Smyth D, Zavitz CC, Shikatani EA, Parsons M, van Rooijen N,

593 Lin HY, Husain M, Libby P, Nahrendorf M, Weissleder R, Swirski FK. 2013. Local  
594 proliferation dominates lesional macrophage accumulation in atherosclerosis. *Nat*  
595 *Med* 19:1166-72.

596 33. Zhu SN, Chen M, Jongstra-Bilen J, Cybulsky MI. 2009. GM-CSF regulates intimal cell  
597 proliferation in nascent atherosclerotic lesions. *J Exp Med* 206:2141-9.

598 34. Ohnmacht C, Pullner A, van Rooijen N, Voehringer D. 2007. Analysis of eosinophil  
599 turnover in vivo reveals their active recruitment to and prolonged survival in the  
600 peritoneal cavity. *J Immunol* 179:4766-74.

601 35. Tesio M, Golan K, Corso S, Giordano S, Schajnovitz A, Vagima Y, Shivtiel S, Kalinkovich  
602 A, Caione L, Gammaitoni L, Laurenti E, Buss EC, Shezen E, Itkin T, Kollet O, Petit I,  
603 Trumpp A, Christensen J, Aglietta M, Piacibello W, Lapidot T. 2011. Enhanced c-Met  
604 activity promotes G-CSF-induced mobilization of hematopoietic progenitor cells via  
605 ROS signaling. *Blood* 117:419-28.

606 36. Vagima Y, Avigdor A, Goichberg P, Shivtiel S, Tesio M, Kalinkovich A, Golan K, Dar A,  
607 Kollet O, Petit I, Perl O, Rosenthal E, Resnick I, Hardan I, Gellman YN, Naor D, Nagler A,  
608 Lapidot T. 2009. MT1-MMP and RECK are involved in human CD34+ progenitor cell  
609 retention, egress, and mobilization. *J Clin Invest* 119:492-503.

610 37. Golan K, Vagima Y, Ludin A, Itkin T, Cohen-Gur S, Kalinkovich A, Kollet O, Kim C,  
611 Schajnovitz A, Ovadya Y, Lapid K, Shivtiel S, Morris AJ, Ratajczak MZ, Lapidot T. 2012.  
612 S1P promotes murine progenitor cell egress and mobilization via S1P1-mediated ROS  
613 signaling and SDF-1 release. *Blood* 119:2478-88.

614 38. Alari-Pahissa E, Notario L, Lorente E, Vega-Ramos J, Justel A, Lopez D, Villadangos JA,  
615 Lauzurica P. 2012. CD69 does not affect the extent of T cell priming. *PLoS One*  
616 7:e48593.

617 39. Cortes JR, Sanchez-Diaz R, Bovolenta ER, Barreiro O, Lasarte S, Matesanz-Marin A,  
618 Toribio ML, Sanchez-Madrid F, Martin P. 2014. Maintenance of immune tolerance by  
619 Foxp3+ regulatory T cells requires CD69 expression. *J Autoimmun* 55:51-62.

620 40. Han Y, Guo Q, Zhang M, Chen Z, Cao X. 2009. CD69+ CD4+ CD25- T cells, a new subset  
621 of regulatory T cells, suppress T cell proliferation through membrane-bound TGF-beta  
622 1. *J Immunol* 182:111-20.

623 41. Sanjabi S, Oh SA, Li MO. 2017. Regulation of the Immune Response by TGF-beta: From  
624 Conception to Autoimmunity and Infection. *Cold Spring Harb Perspect Biol* 9.

625 42. Powell JD, Pollizzi KN, Heikamp EB, Horton MR. 2012. Regulation of immune responses  
626 by mTOR. *Annu Rev Immunol* 30:39-68.

627 43. Maeurer C, Holland S, Pierre S, Potstada W, Scholich K. 2009. Sphingosine-1-phosphate  
628 induced mTOR-activation is mediated by the E3-ubiquitin ligase PAM. *Cell Signal*  
629 21:293-300.

630 44. Liu G, Yang K, Burns S, Shrestha S, Chi H. 2010. The S1P(1)-mTOR axis directs the  
631 reciprocal differentiation of T(H)1 and T(reg) cells. *Nat Immunol* 11:1047-56.

632 45. Smith GL, Benfield CT, Maluquer de Motes C, Mazzon M, Ember SW, Ferguson BJ,  
633 Sumner RP. 2013. Vaccinia virus immune evasion: mechanisms, virulence and  
634 immunogenicity. *J Gen Virol* 94:2367-92.

635

636 **Figure legends**

637 **Figure 1. HuCD69 mice treated with the mAb anti-huCD69-2.8 exhibited a higher**  
638 **antiviral response several days after vaccinia virus infection than control-treated mice.** A-  
639 F, Mice were treated with PBS or 200 µg of anti-huCD69-2.8 with two doses separated by one  
640 week. Five days after the second treatment, the mice were infected with  $1 \times 10^7$  pfu administered  
641 i.p, and 7 days after infection, the mice were analyzed. B, Viral titers in the ovaries were  
642 measured. C, Absolute cell numbers in the spleen, bone marrow, lymph nodes and blood were  
643 measured. D, The numbers of different lymphoid and myeloid cell populations in the spleen  
644 were measured. E-F, The numbers of IFN $\gamma$  and TNF $\alpha$ -producing cells in the spleen were  
645 measured. Two independent experiments were pooled, with a total of n=8 mice per group. G,H.  
646 Mice were treated with PBS or 500ug of anti-huCD69 2.8 and one day after were infected  
647 intranasally with  $1 \times 10^5$  pfu of VACV-WR. One week after infection, mice received a second  
648 dose of treatment. Weight loss was evaluated over 9 days. Data shown are representative of one  
649 experiment with n=5-6 mice per group. Data were analyzed by unpaired *t* test, where \*= $p \leq 0.05$ ,  
650 \*\*= $p \leq 0.01$ , \*\*\*= $p \leq 0.001$ , and \*\*\*\*= $p \leq 0.0001$ .

651

652 **Figure 2. Early anti-VACV response upon targeting CD69 with the anti-huCD69- 2.8 mAb**  
653 **promoted better viral clearance and a concomitant accumulation of leukocytes two days**  
654 **after infection.** A, Mice were treated with 2 doses of 200 µg of anti-huCD69-2.8 or PBS  
655 administered i.v with the doses separated by 1 week, and 5 days after the second dose, the mice  
656 were infected with VACV and analyzed 2 days after infection. B, Viral titers in the ovaries were  
657 measured. C, Absolute cell numbers in the spleen, bone marrow, lymph nodes, thymus and  
658 blood were measured. D, The numbers of leukocyte subpopulations in the spleen were  
659 measured. E-F, The numbers of IFN $\gamma$ - and TNF $\alpha$ -producing cells in the spleen were measured.  
660 G, Mice were treated with 1 dose of 500 µg of anti-huCD69-2.8 or PBS administered i.v and 24  
661 hours after treatment, the mice were infected with VACV i.v and viral titers were analyzed 6  
662 hours after infection. Viral titers in spleen were measured. B-F, Two independent experiments  
663 were pooled, with a total of n=7 mice per group. G, One experiment with n=4-5 mice per group.  
664 Data were analyzed by an unpaired *t* test, where \*= $p \leq 0.05$ , \*\*= $p \leq 0.01$ , \*\*\*= $p \leq 0.001$  and  
665 \*\*\*\*= $p \leq 0.0001$ .

666

667 **Figure 3. Immunocompetent mice treated with the anti-mCD69-2.2 mAb exhibited better**  
668 **viral clearance.** A, Mice were treated with 1 dose of 500 µg of anti-mCD69- 2.2 mAb or PBS  
669 administered i.v 24 hours before infection with VACV and analyzed 2 days after infection. B,  
670 Viral titers in the ovaries were measured. C, Absolute cell numbers in the spleen, bone marrow,  
671 lymph nodes, thymus and blood were measured. D, The numbers of leukocyte subpopulations in

672 the spleen were measured. E-F, The percentages and G-H, numbers of IFN $\gamma$ - and TNF $\alpha$ -  
673 producing cells in the spleen were measured. I, Mice were infected with 10<sup>7</sup> pfu of VACV and  
674 one day after were treated with 500  $\mu$ g of anti-mCD69- 2.2 mAb or PBS administered i.v 24  
675 hours. Viral titers were analyzed 2 days after infection. J, Viral titers were measured in ovaries.  
676 B-H, Two independent experiments were pooled, with a total of n $\geq$ 7 mice per group. J, One  
677 experiment with n=4 mice per group. Data were analyzed by an unpaired t test, where  
678 \*=p $\leq$ 0.05, \*\*=p $\leq$ 0.01, \*\*\*=p $\leq$ 0.001, and \*\*\*\*=p $\leq$ 0.0001.

679

680 **Figure 4. mAb anti-mCD69 2.2 treatment in Rag2<sup>-/-</sup> CD69<sup>+/+</sup> mice induced an increased**  
681 **accumulation of leukocytes and promoted NK cell activity.** A, Mice were treated with anti-  
682 mCD69-2.2 or PBS with two doses separated by one week; 5 days after the second treatment,  
683 the mice were infected with 1x10<sup>6</sup> pfu administered i.p, and two days after infection, the mice  
684 were sacrificed. B, Viral titers were measured. C, Absolute cell numbers in the spleen, thymus,  
685 bone marrow and blood were compared between anti-mCD69-2.2-treated mice and untreated  
686 mice. D-E, Lymphoid and myeloid subpopulation cell numbers were analyzed in the D, bone  
687 marrow and E, spleen. F, and G, The intracellular production of IFN- $\gamma$  and TNF $\alpha$  and surface  
688 expression of CD107a in NK cells were measured. B, One experiment representative of two  
689 independent experiments is shown. C-H, Three independent experiments were pooled, with a  
690 total of n $\geq$ 8 mice per group. Data were analyzed by an unpaired t test, where \*=p $\leq$ 0.05,  
691 \*\*=p $\leq$ 0.01, \*\*\*=p $\leq$ 0.001 and \*\*\*\*=p $\leq$ 0.0001.

692

693 **Figure 5. HuCD69 mice treated with two doses of an anti-human CD69 antibody showed**  
694 **similar effects on the cell numbers of the bone marrow and spleen compared to mice given**  
695 **a one-dose treatment.** A and B, Mice were treated with two doses of 200  $\mu$ g of anti-huCD69-  
696 2.8 separated by one week, and five days after the second treatment, the mice were analyzed. A,  
697 Total cell number. B, Numbers of lymphoid and myeloid subpopulation cells in the spleen. Two  
698 independent experiments were pooled, with a total of n $\geq$ 8 mice per group. Data were analyzed  
699 by an unpaired t test, where \*=p $\leq$ 0.05, \*\*=p $\leq$ 0.01, \*\*\*=p $\leq$ 0.001 and \*\*\*\*=p $\leq$ 0.0001.

700

701 **Figure 6. Treatment with anti-human-CD69-2.8 antibody increased proliferation and**  
702 **survival in the spleen.** A-B, Mice were treated or not treated with 500  $\mu$ g of anti-huCD69-2.8  
703 24 hours before a BrdU injection. The mice received 1 mg of BrdU intraperitoneally, and, three  
704 hours later, were sacrificed. BrdU incorporation was assessed in the lymphoid and myeloid  
705 subpopulations of the BM (A) and spleen (B) by flow cytometry. C. Survival was measured by  
706 PI staining of unfractionated splenocytes from uninfected HuCD69 mice treated with the anti-  
707 huCD69-2.8 mAb or an isotype control. A-B, Two independent experiments were pooled, with  
708 a total of n $\geq$ 8 mice per group. C, One independent experiment representative of two

709 experiments is shown. Data were analyzed by an unpaired t test, where  $*=p\leq 0.05$ ,  $**=p\leq 0.01$ ,  
710  $***=p\leq 0.001$  and  $****=p\leq 0.0001$ .

711

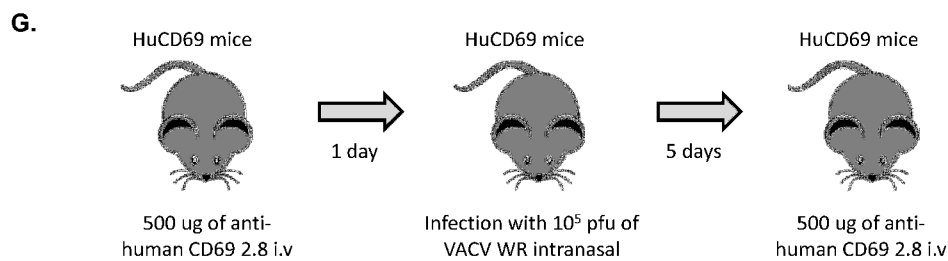
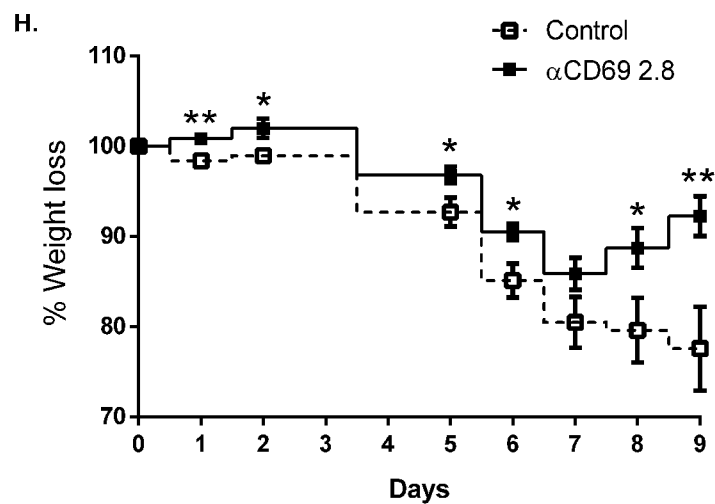
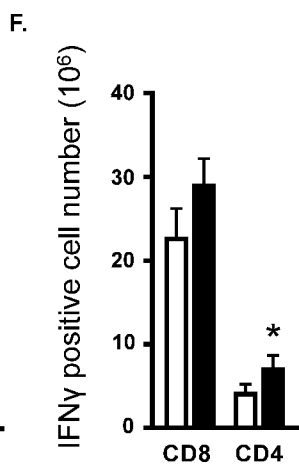
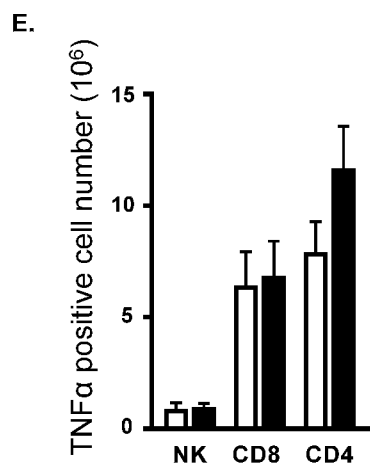
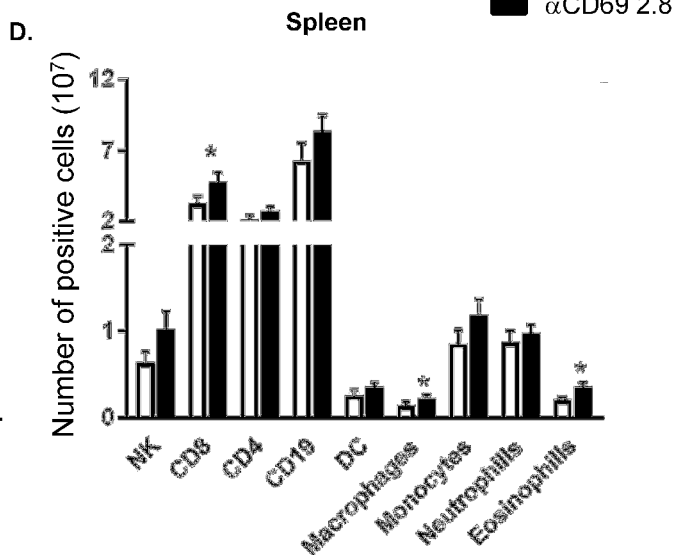
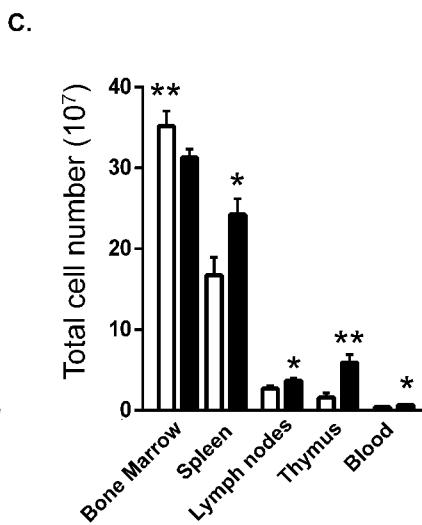
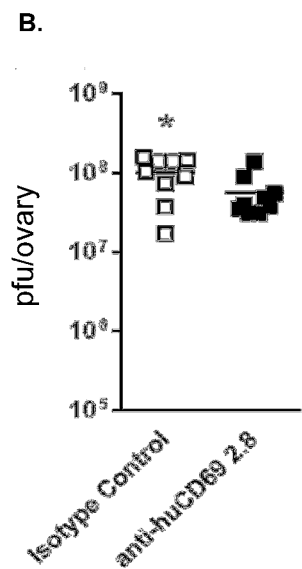
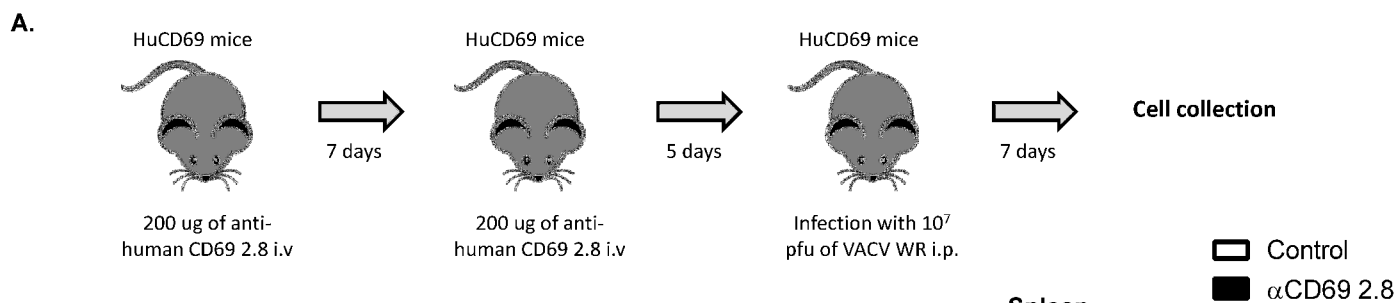
712 **Figure 7. Targeting human CD69 promoted an increase in the levels of some**  
713 **proinflammatory cytokines.** A-C, Mice were treated or not treated with 500  $\mu\text{g}$  of anti  
714 huCD69-2.8 24 hours before analysis. A, IL-2 and CD25 expression were measured in the bone  
715 Marrow, spleen and blood by flow cytometry. B, The relative mRNA expression of TGF- $\beta$  was  
716 compared between treated and control mice. C, The protein levels of certain cytokines in  
717 supernatants of splenocytes was measured by Luminex assay. D-G, Splenocytes were collected  
718 from mice treated with 500  $\mu\text{g}$  of anti-huCD69-2.8 for 24 hours or left untreated. D-E, mRNA  
719 of proinflammatory cytokines and their receptors were assayed through an array. D, data for IL-  
720 17a, IL-17b, IL-17f, IL1- $\alpha$ , IL-1 $\beta$ , LTa, LTb and IFN $\gamma$  are shown. E, Data for CCL2 and CCL12  
721 are shown. Data are represented in a graph as the fold-induction relative to the  $\beta$ -actin level. F,  
722 qPCR analysis of IL-17f, IL1-  $\alpha$ , IL-1 $\beta$ , TNF $\alpha$  and IL-21 is shown. G, qPCR analysis of CCL2  
723 and CCL12 is shown.

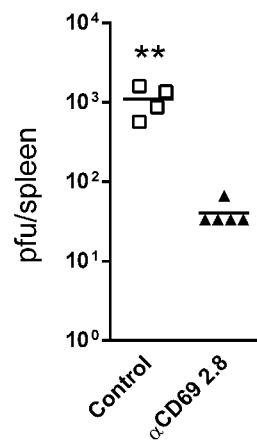
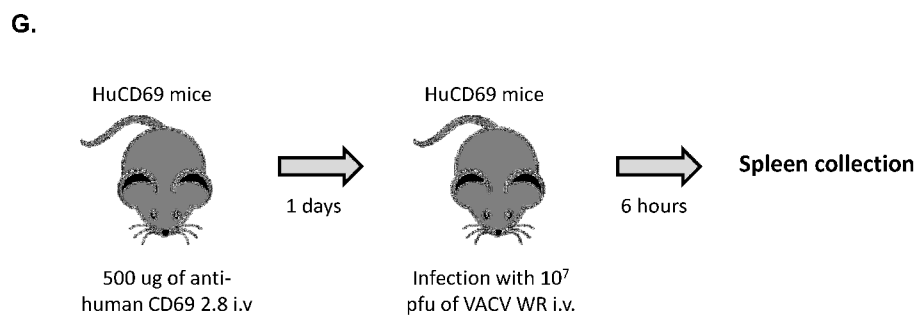
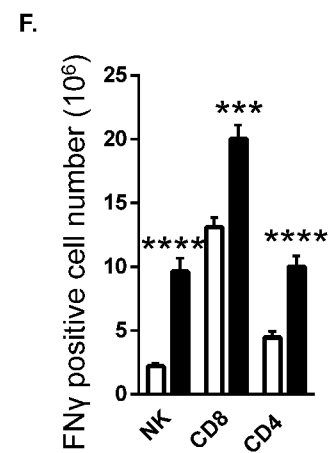
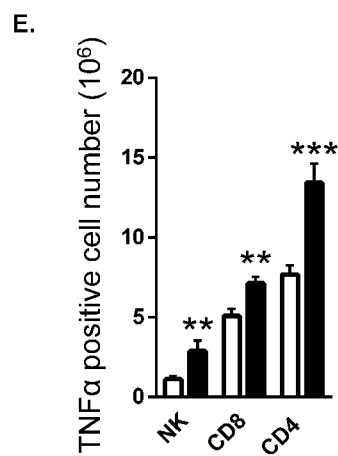
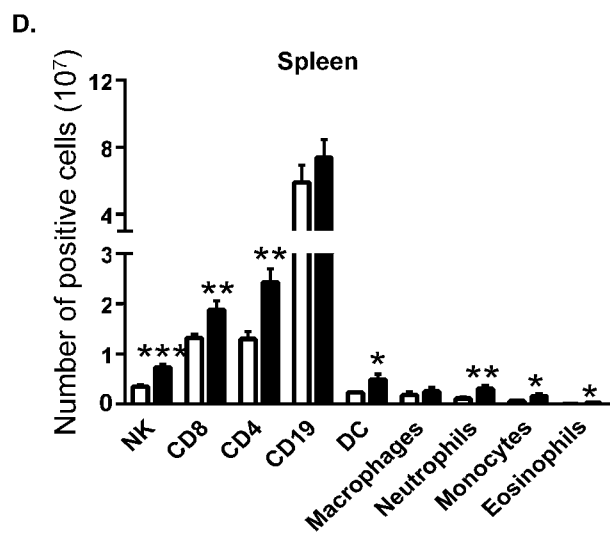
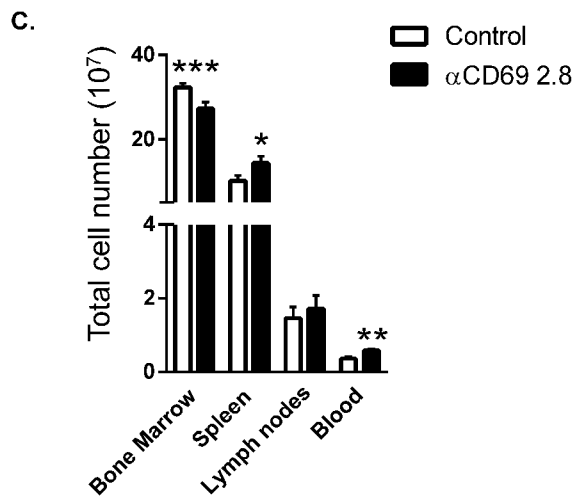
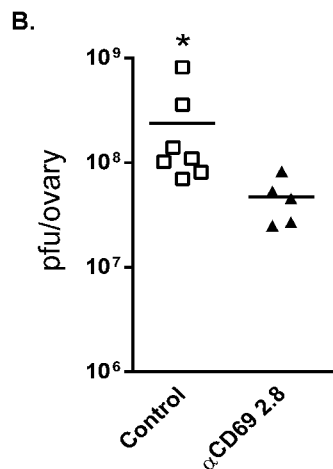
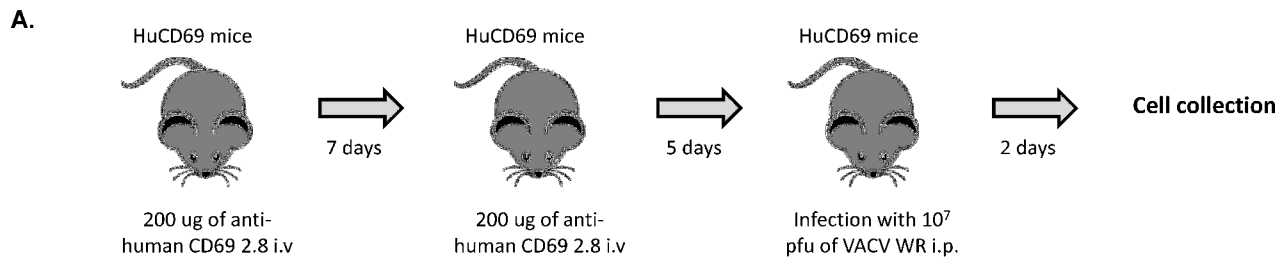
724 A, Three experiments were pooled, with a total of  $n\geq 10$  mice per group. B, One experiment is  
725 shown. C, Four independent experiments were pooled, with a total of  $n\geq 12$  mice per group. D-  
726 G, One experiment is shown with samples pooled of two or three experiments. Data were  
727 analyzed by an unpaired t test, where  $*=p\leq 0.05$ ,  $**=p\leq 0.01$ ,  $***=p\leq 0.001$  and  $****=p\leq 0.0001$ .

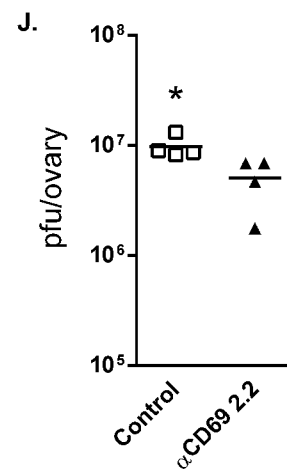
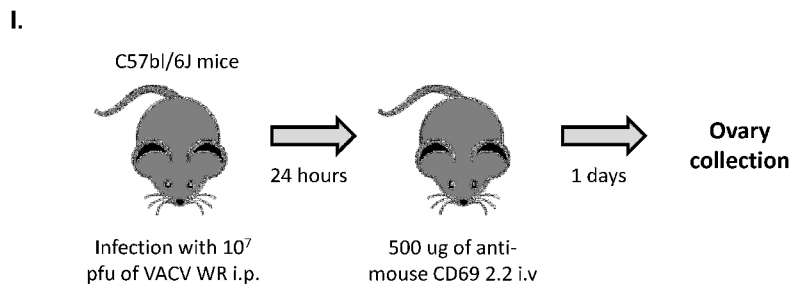
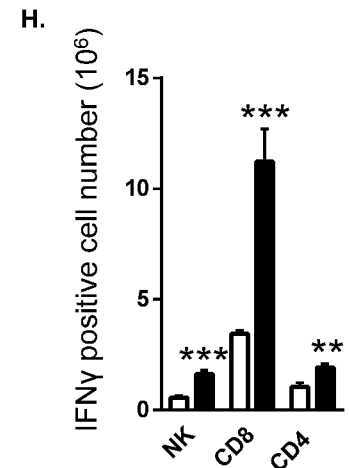
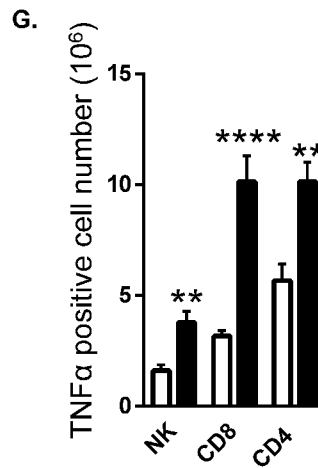
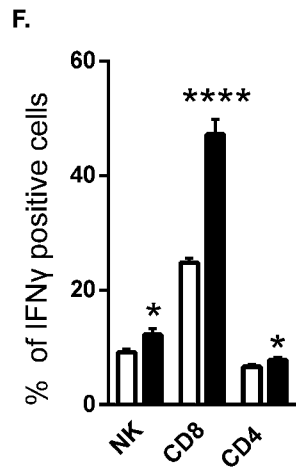
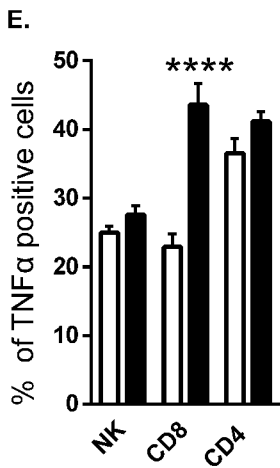
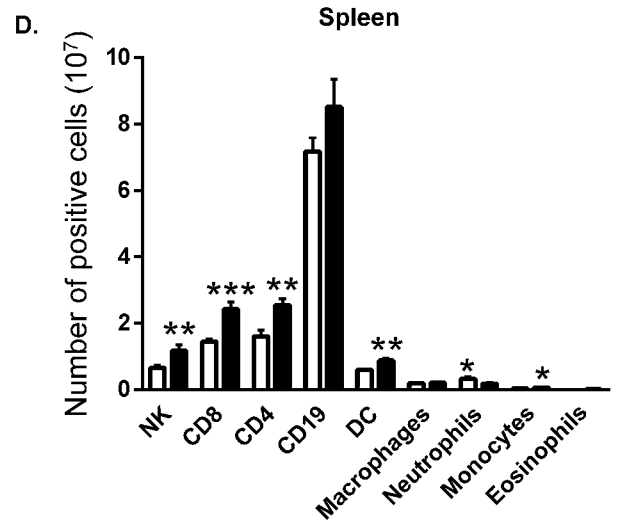
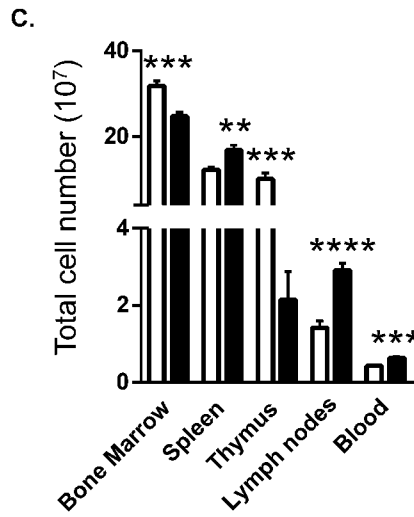
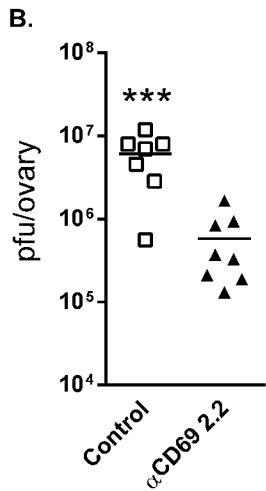
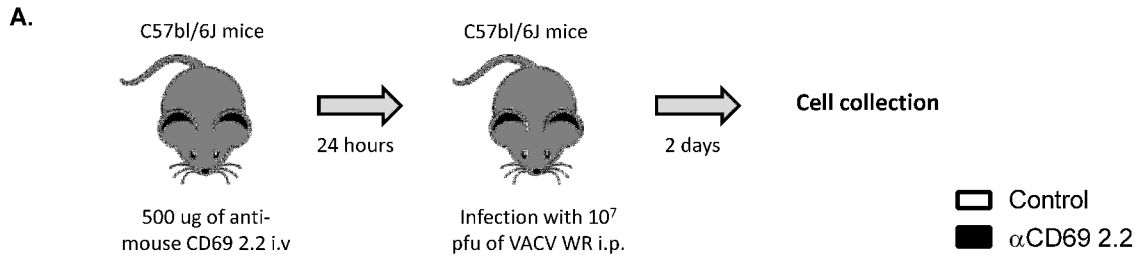
728

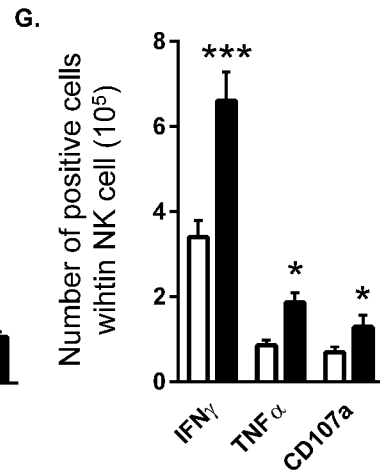
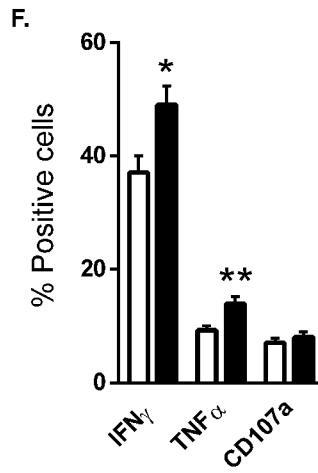
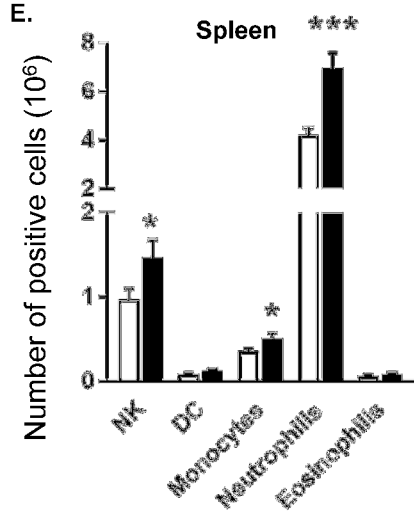
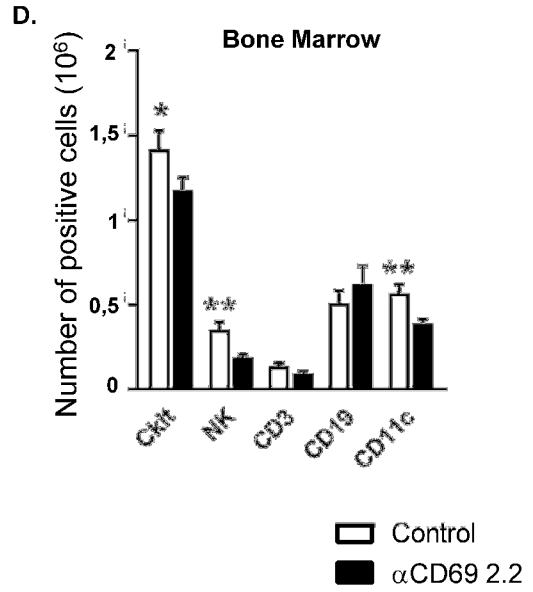
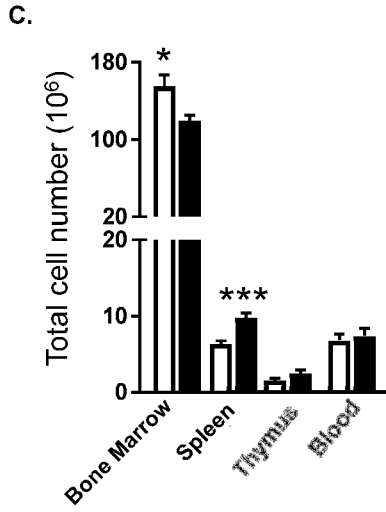
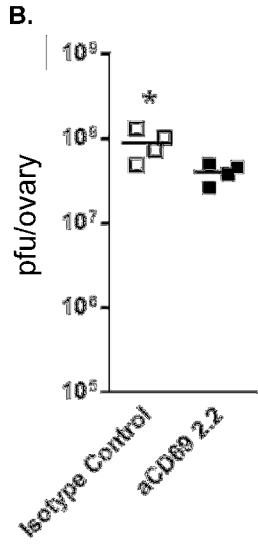
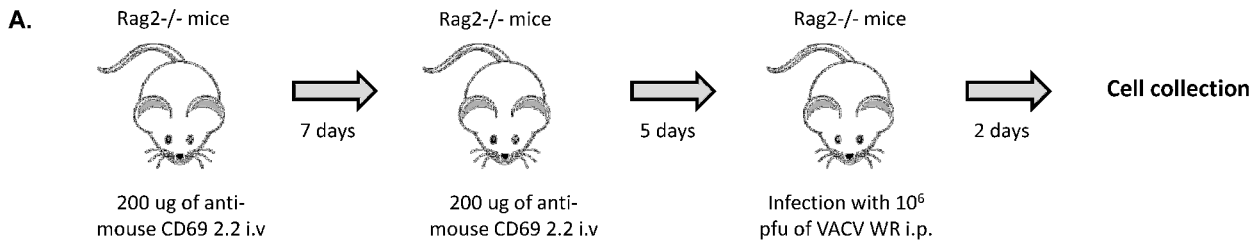
729 **Figure 8. Targeting human CD69 induced increased splenic cellularity mediated by**  
730 **mTOR.** A-C, Mice were treated with 500  $\mu\text{g}$  of anti-huCD69-2.8 administered i.v 24 hours  
731 before analysis, 480 mg of rapamycin/kg administered i.p for five days or both, as indicated. A,  
732 The total cell numbers in the spleen (left) and bone marrow (right) are shown. B, p70, S6K and  
733 S6 phosphorylation was assessed by immunoblotting splenocyte extracts from the indicated  
734 mice. C, Mice were treated with two doses of FTY720 (5 mg/kg) administered i.p and separated  
735 by 24 hours; 6 hours after the first dose of FTY720, the mice were treated with 500  $\mu\text{g}$  of anti-  
736 huCD69-2.8 administered i.v. as appropriate, and 24 hours after anti-huCD69-2.8 injection, the  
737 mice were analyzed. mTOR and S6 phosphorylation was assessed by immunoblotting  
738 splenocyte extracts. A, Two independent experiments were performed. B-C, One experiment  
739 was performed. Data were analyzed by an unpaired t test, where  $*=p\leq 0.05$ ,  $**=p\leq 0.01$ ,  
740  $***=p\leq 0.001$  and  $****=p\leq 0.0001$ .

741

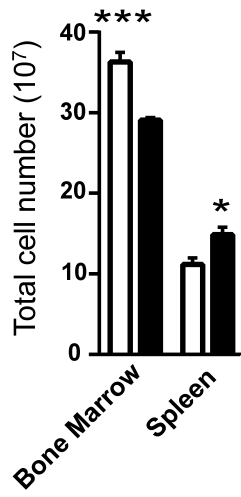




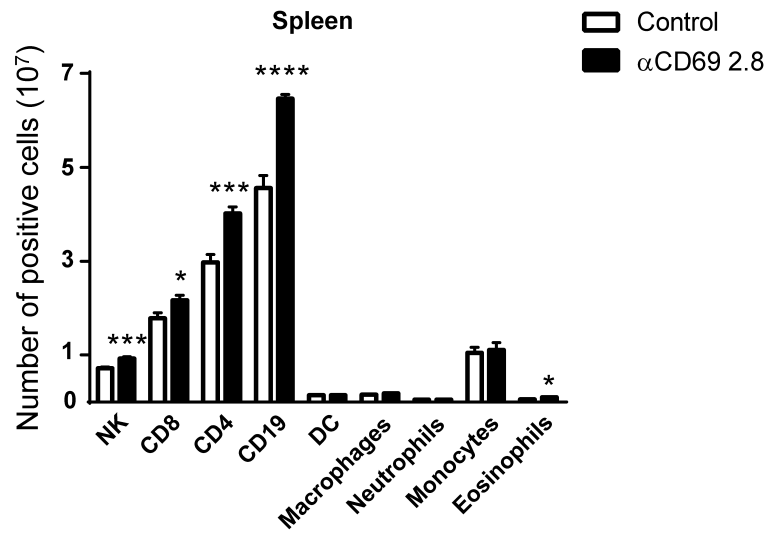




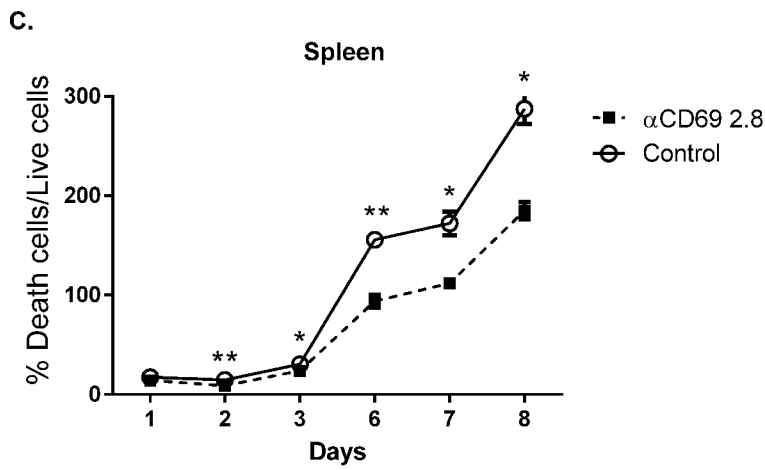
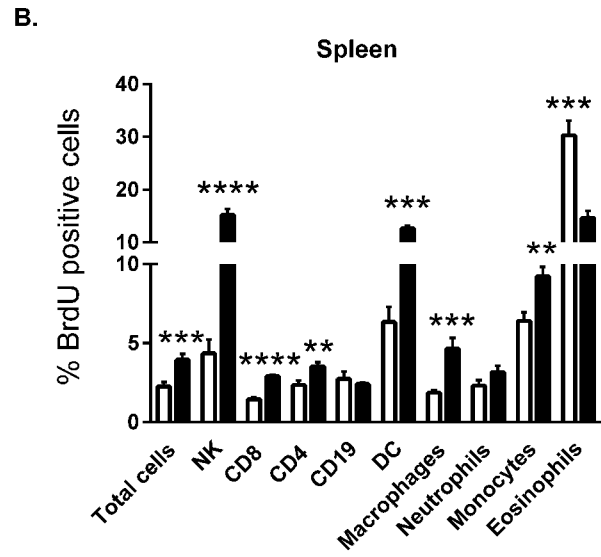
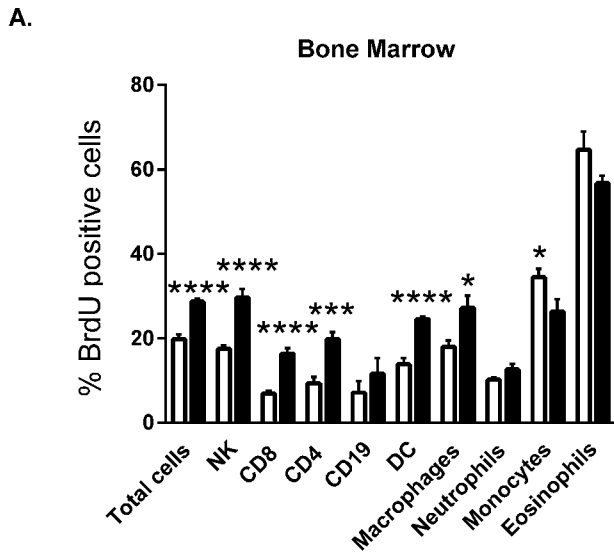
A.

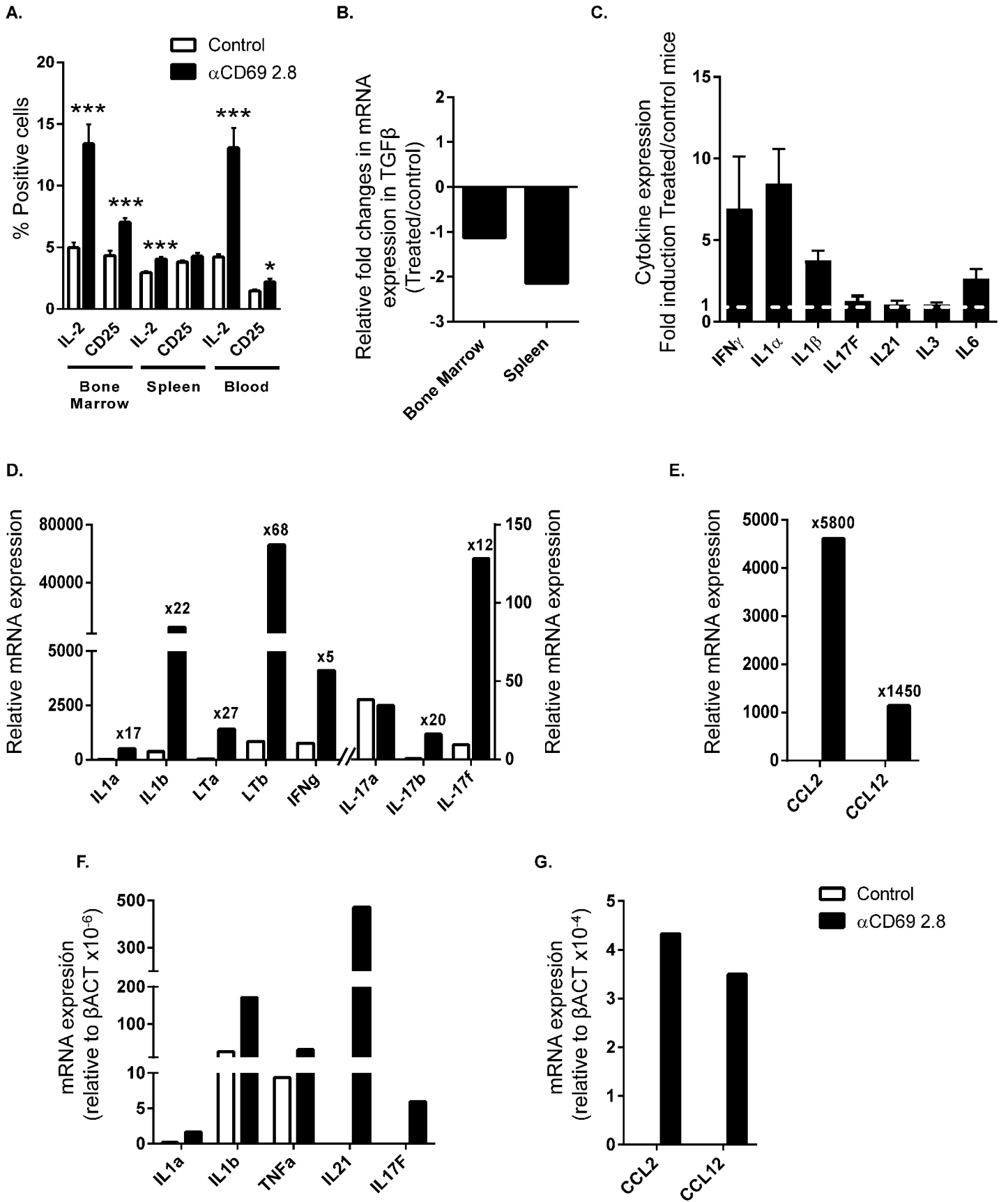


B.

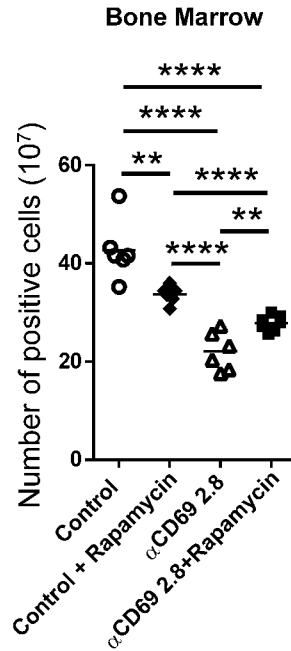
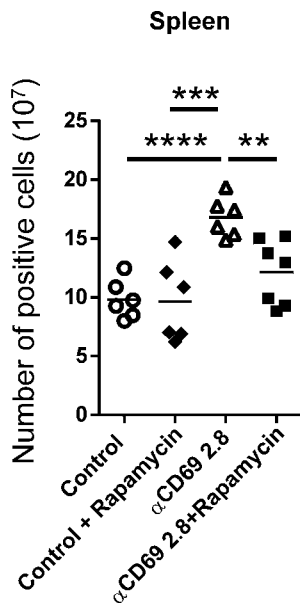


Control  
  $\alpha$ CD69 2.8

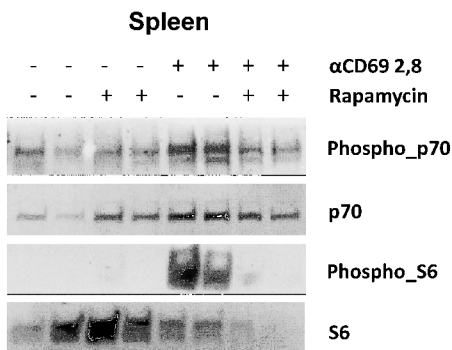




A.



B.



C.

